Polyhedron 52 (2013) 482–490

Contents lists available at SciVerse ScienceDirect

Polyhedron

journal homepage: www.elsevier.com/locate/poly

Salts with the $[NiBr_3(L)]^-$ complex anion (L = 1-methylimidazole, 1-methylbenzimidazole, quinoline, and triphenylphosphane) and low melting points: A comparative study

Tim Peppel [1], Alexander Hinz, Martin Köckerling *

Institute of Chemistry, Inorganic-Solid State Chemistry Group, University of Rostock, Albert-Einstein-Str. 3a, D-18059 Rostock, Germany

ARTICLE INFO

Article history:
Available online 8 September 2012

Dedicated on the Occasion of the 100th Anniversary of the 1913 Noble Prize in Chemistry to Alfred Werner.

Keywords:
Nickel complexes
N ligand
Bromide
X-ray structure
Thermal properties
Spectroscopy

ABSTRACT

Four new salts with low melting points of the general formula $(EMIm)[NiBr_3(L)]$ (EMIm = 1-ethyl-3-methyl-imidazolium) with L = *N*-methylimidazole (NMIm), *N*-methylbenzimidazole (NMBIm), quinoline (quin), and triphenylphosphane (PPh_3) were prepared and characterized by means of elemental analysis, IR, NMR, and UV–vis spectroscopy. Magnetic properties were deduced from NMR data using the EVANS method. All four compounds are paramagnetic with magnetic moments close to the spin-only values of the tetrahedrally coordinated Ni(II) ion. Molecular and crystal structures were obtained by single crystal X-ray diffraction investigations. Melting points are determined to have values between 110 °C, $(EMIm)[NiBr_3(NMIm)]$ and 168 °C, $(EMIm)[NiBr_3(PPh_3)]$. They exceed the maximum temperature required to call them "Ionic Liquids". Decomposition has been found to occur above 200 °C and to depend largely on the type of organic ligand coordinated to Ni(II).

1. Introduction

Solids with low melting points have found many applications as reaction media for the production of a wide range of materials. Especially the so-called Ionic Liquids have been in the focus of interest for their unique properties for more than two decades. Characteristics are melting points below 100 °C, wide temperature ranges wherein the salts are liquid, low vapor pressures, and high electric conductivities [1], to name just a few. Paramagnetic complex anions incorporated in Ionic Liquids result in substances with the intriguing combination of properties of being both liquid and responding to magnetic fields [2]. The work of Hayashi et al. on $[FeCl_4]^-$ containing Ionic Liquids [2] boosted research on transition metal containing Ionic Liquids, because of numerous possible applications, like transport and materials separation [2e], catalysis [2f] or field dependent absorption [2g], to name a few. An example of a similar paramagnetic ion is that of the general formula $[MX_3(quin)]^-$ (M = 3d-metal; X = Cl, Br, I; quin = quinoline) which is known for Mn(II) [3], Fe(II) [4], Co(II) [5], Ni(II) [2c,6], Cu(II) [7], and Zn(II) [8]. Preparative investigations were conducted in our laboratories to find cation combinations with such anions with low melting points. Recently, we have investigated a series of Ionic Liquids containing the $[CoBr_3(quin)]^-$ anion [9]. To get a better understanding of the relation between thermal properties and solid state characteristics the neutral ligand in this type of anion is varied.

In this contribution we report on the syntheses, properties, and structures of a series of $(EMIm)[NiBr_3(L)]$ salts (EMIm = 1-ethyl-3-methyl-imidazolium) with L = *N*-methylimidazole (NMIm), *N*-methylbenzimidazole (NMBIm), quinoline (quin), and triphenylphospane (PPh_3)).

2. Experimental

2.1. Materials and methods

N-Methylimidazole, quinoline, benzimidazole, iodomethane and anhydrous $NiBr_2$ were purchased from Sigma–Aldrich (>99%) and used as received. *N*-Methyl-benzimidazole was synthesized according to a known literature method [10]: Benzimidazole (25.0 g, 211.6 mmol) is added in one portion to 100 mL of a stirred ice-cold 50% aqueous NaOH solution. Iodomethane (33.0 g, 232.8 mmol) is added dropwise under vigorous stirring to the clear benzimidazole solution at ambient temperature. After 1 h the solution is extracted three times with 100 mL portions of chloroform. The combined organic phases are dried with Na_2SO_4 and the solvent is removed under reduced pressure. The residue is distilled

---

* Corresponding author. Tel.: +49 (0)381 4986390; fax: +49 (0)381 4986382.
E-mail address: Martin.Koeckerling@uni-rostock.de (M. Köckerling).

[1] Present address: Leibniz Institute for Catalysis, Albert-Einstein-Str. 29a, D-18059 Rostock, Germany.

0277-5387/$ - see front matter © 2012 Elsevier Ltd. All rights reserved.
http://dx.doi.org/10.1016/j.poly.2012.08.047

Table 1
Crystal data and structure refinement parameters for (EMIm)[NiBr$_3$(L)], with L = NMIm, NMBIm, quin, and PPh$_3$.

L	NMIm	NMBIm	Quin	PPh$_3$
Formula	$C_{10}H_{17}Br_3N_4Ni$	$C_{14}H_{19}Br_3N_4Ni$	$C_{15}H_{18}Br_3N_3Ni$	$C_{24}H_{26}Br_3N_2NiP$
Formula weight	491.72	541.77	538.76	671.88
T (K)	173(2)	173(2)	173(2)	173(2)
Crystal system	monoclinic	monoclinic	triclinic	triclinic
Space group	$P2_1/n$ (No. 14)	$P2_1/c$ (No. 14)	$P\bar{1}$(No. 2)	$P\bar{1}$(No. 2)
Z	4	4	2	2
Unit cell dimensions				
a (Å)	7.742(2)	13.8876(4)	7.4845(5)	10.4387(2)
b (Å)	14.506(3)	10.4570(3)	8.1975(6)	11.0013(2)
c (Å)	14.843(3)	12.9338(3)	15.204(1)	13.8378(2)
α (°)	90	90	88.331(5)	79.131(1)
β (°)	92.01(3)	92.165(1)	85.297(5)	71.119(1)
V (Å^3)	1665.9(6)	1876.94(9)	913.2(1)	1331.83(4)
$\rho_{calc.}$ (g·cm^{-3})	1.961	1.917	1.959	1.675
μ (mm^{-1})	8.349	7.421	7.624	5.303
λ (Å)	0.71073	0.71073	0.71073	0.71073
No. parameters	164	200	200	290
Goodness-of-fit (GOF) on F^2	1.021	1.028	1.052	1.039
Final R indices [$I > 2\sigma(I)$][a,b]	$R1 = 0.0381$, $wR2 = 0.0663$	$R1 = 0.0223$, $wR2 = 0.0488$	$R1 = 0.0326$, $R2 = 0.0714$	$R1 = 0.0327$, $wR2 = 0.0719$
Weighting A/B[c]	0.0225/1.1862	0.0220/1.0026	0.0339/0.6411	0.0335/0.4157

[a] $R1 = \sum \|\|F_o\| - \|F_c\|\| / \sum \|F_c\|$.

[b] $wR2 = \sqrt{\left[\sum\{w(F_o^2 - F_c^2)^2\} / \sum\{w(F_o^2)^2\}\right]}$.

[c] $w = 1/[\sigma_2(F_0^2) + (A \cdot P)^2 + B \cdot P]$; $P = (F_0^2 + 2F_c^2)/3$.

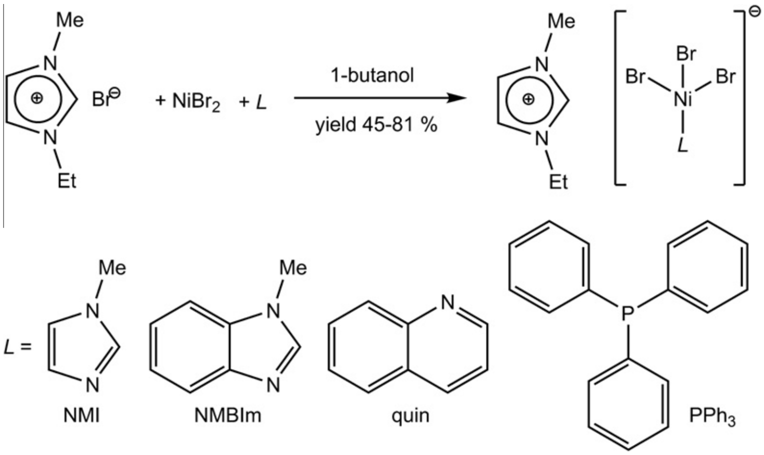

Scheme 1. Reaction sequence for the synthesis of (EMIm)[NiBr$_3$(L)].

in vacuo, yielding *N*-methyl-benzimidazole as a colorless liquid, which solidifies upon cooling. Yield: 21.0 g (75%), mp. 61 °C. Elemental anal. % (calc. for $C_8H_8N_2$): C, 72.50 (72.70); H, 6.19 (6.10); N, 21.18 (21.20).

2.2. General synthesis of (EMIm)[NiBr$_3$(L)] (L = NMIm, NMBIm, quin, PPh$_3$)

1-Ethyl-3-methylimidazolium bromide ((EMIm)Br, 0.9 g, 4.7 mmol) and appropriate ligand L (4.7 mmol; PPh$_3$: 1.2 g, quin: 0.6 g, NMIm: 0.4 g, NMBIm: 0.6 g) are dissolved in 25 mL of hot 1-butanol and added to a vigorously stirred boiling suspension of NiBr$_2$ (1.0 g, 4.6 mmol) in 25 mL of the same solvent. The resulting mixture turns dark blue immediately and the desired product precipitates in form of crystals upon storing the solution at 0 °C overnight. The precipitate is filtered off, washed with diethyl ether and finally dried *in vacuo* at ambient temperature.

(EMIm)[NiBr$_3$(PPh$_3$)]: Yield: 2.5 g, 81%, mp. 168 °C. Elemental anal. % (calc. for $C_{24}H_{26}Br_3N_2NiP$): C, 42.59 (42.90); H, 3.89 (3.90); N, 4.26 (4.17). UV–vis (λ_{max}/nm in acetonitrile, 25 °C): 378 (~390) , 640 (~685). IR (ν_{max}/cm^{-1}): 3144w, 3105w, 3084w, 3053w, 2978w, 2932w, 1584vw, 1568m, 1481m, 1462w, 1435s, 1387w, 1353vw, 1336w, 1315w, 1291w, 1267vw, 1247vw, 1185w, 1167s, 1120w, 1097s, 1073w, 1028w, 995w, 959vw, 932vw, 921vw, 837m, 795w, 756s, 745s, 709m, 693s, 647m, 617s, 594w. Magnetic data: $\mu_{eff}/\mu_B = 3.76$ (T = 25 °C, $c = 2.13 \cdot 10^{-2}$ mol/L, ν_0 = 300 MHz, $\chi_{mol} = 5.93 \cdot 10^{-3}$).

(EMIm)[NiBr$_3$(quin)]: Yield: 1.5 g, 61%, mp. 124 °C. Elemental anal. % (calc. for $C_{15}H_{18}Br_3N_3Ni$): C, 33.47 (33.44); H, 3.37 (3.37); N, 7.67 (7.80). UV–vis (λ_{max}/nm in acetonitrile, 25 °C): 372, 620, 649, 700. IR (ν_{max}/cm^{-1}): 3144w, 3106w, 3080m, 3016vw, 2980w, 2952vw, 2882vw, 2828vw, 1622w, 1593w, 1583vw, 1570m, 1509s, 1455w, 1438w, 1397w, 1377 m, 1342w, 1311m, 1281vw, 1258w, 1234w, 1200w, 1165s, 1127w, 1097vw, 1089w, 1057w, 1026w, 991w, 957m, 866w, 848m, 813s, 779s, 754s, 733s, 708w, 645vw, 636 m, 619s, 529w. Magnetic data: $\mu_{eff}/\mu_B = 3.76$ (T = 25 °C, $c = 2.83 \cdot 10^{-2}$ mol/L, ν_0 = 300 MHz, $\chi_{mol} = 5.92 \cdot 10^{-3}$).

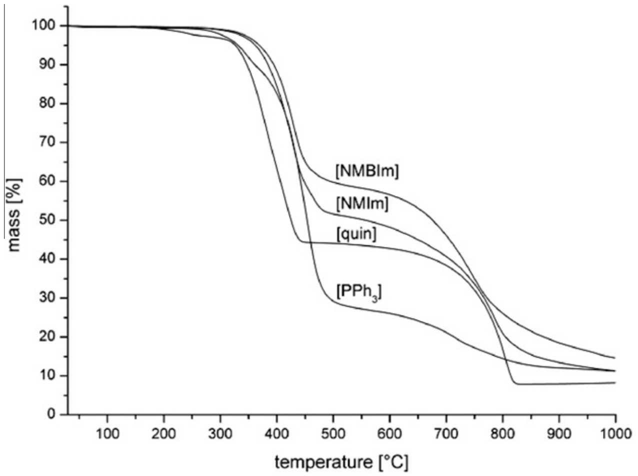

Fig. 1. TGA curves of (EMIm)[NiBr$_3$(*L*)] in the temperature range of 30–1000 °C in air (*L* is given in squared brackets).

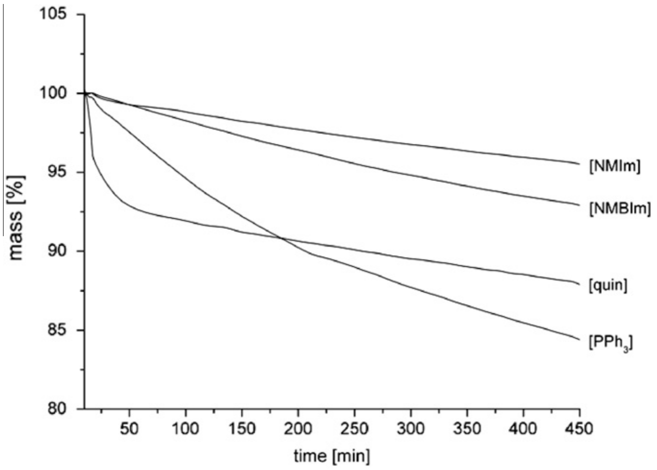

Fig. 2. Isothermal TGA curves of (EMIm)[NiBr$_3$(*L*)] at 200 °C in air (*L* is given in squared brackets).

Table 2
Selected bond lengths in Å and angles in ° of the compounds (EMIm)[NiBr$_3$(*L*)] with *L* = NMIm, NMBIm, quin, and PPh$_3$.

L	NMIm	NMBIm	Quin	PPh$_3$
Atom distances				
Ni1-Br1	2.3723(3)	2.3883(8)	2.4035(6)	2.3614(4)
Ni1-Br2	2.3857(3)	2.3848(6)	2.3837(5)	2.3742(3)
Ni1-Br3	2.3990(3)	2.3833(8)	2.3795(6)	2.3651(3)
Average Ni1-Br	2.3857(3)	2.3855(7)	2.3899(6)	2.3669(4)
Ni1-L	1.973(2)	1.974(2)	2.021(3)	2.3016(6)
Bond angles				
Br1-Ni1-Br2	122.93(2)	116.46(1)	106.68(2)	117.31(1)
Br1-Ni1-Br3	104.82(2)	113.63(1)	114.66(2)	111.79(1)
Br2-Ni1-Br3	113.36(2)	110.48(1)	110.22(2)	112.70(1)
Average Br-Ni1-Br	113.70(2)	113.52(2)	110.52(2)	113.93(1)
L-Ni1-Br1	106.06(7)	104.37(5)	99.72(8)	103.51(2)
L-Ni1-Br2	105.50(6)	106.89(5)	121.41(8)	102.78(2)
L-Ni1-Br3	102.56(7)	103.76(5)	104.36(8)	107.17(2)
Average L-Ni1-Br	104.71(7)	105.01(5)	108.50(8)	104.49(2)

Table 3
Absorption maxima in the UV–vis spectra in nm for the compounds (EMIm)[NiBr$_3$(*L*)] with *L* = NMIm, NMBIm, quin, and PPh$_3$.

L	NMIm	NMBIm	Quin	PPh$_3$
$\lambda_{max}(1)$	350	355	372	378
$\lambda_{max}(2)$	621	602	649	640

(EMIm)[NiBr$_3$(NMIm)]: Yield: 1.0 g, 45%, mp. 110 °C. Elemental anal. % (calc. for $C_{10}H_{17}Br_3N_4Ni$): C, 24.58 (24.43); H, 3.82 (3.49); N, 11.26 (11.40). UV–vis (λ_{max}/nm in acetonitrile, 25 °C): 267, 350, 621. IR (ν_{max}/cm^{-1}): 3140w, 3121vw, 3105m, 2981w, 2944vw, 1699w, 1614w, 1569m, 1538w, 1524w, 1505vw, 1468w, 1454w, 1422w, 1387vw, 1342w, 1317w, 1285w, 1271vw, 1235m, 1170s, 1135vw, 1102s, 1095s, 1033vw, 1023vw, 956w, 855m, 834s, 799vw, 765m, 751s, 707w, 670w, 657m, 618s. Magnetic data: $\mu_{eff}/\mu_B = 3.75$ ($T = 25$ °C, $c = 5.66 \cdot 10^{-2}$ mol/L, $\nu_0 = 300$ MHz, $\chi_{mol} = 5.91 \cdot 10^{-3}$).

(EMIm)[NiBr$_3$(NMBIm)]: Yield: 1.8 g, 71%, mp. 150 °C. Elemental anal. % (calc. for $C_{14}H_{19}Br_3N_4Ni \cdot 0.3BuOH$): C, 32.47 (32.37); H, 3.74 (3.93); N, 10.16 (9.93). UV–vis (λ_{max}/nm in acetonitrile, 25 °C): 320, 360, 602. IR (ν_{max}/cm^{-1}): 3152vw, 3121vw, 3105w, 3078w, 3030vw, 2982vw, 2952vw, 1765w, 1732w, 1616w, 1293w, 1574w, 1567vw, 1557vw, 1538vw, 1522 m, 1485w, 1456m, 1421w, 1368w, 1339w, 1296m, 1253m, 1195vw, 1189w, 1170w, 1135w, 1095vw, 1070w, 1031vw, 1007w, 970vw, 926w, 905vw, 886vw, 869w, 848w, 775w, 761w, 738s, 667vw, 629vw, 618m, 5875w, 525w. Magnetic data: $\mu_{eff}/\mu_B = 3.72$ ($T = 25$ °C, $c = 4.97 \cdot 10^{-2}$ mol/L, $\nu_0 = 300$ MHz, $\chi_{mol} = 5.80 \cdot 10^{-3}$).

2.3. Structure analysis and refinement

Transparent, blue single crystals of the four title compounds were selected and separated with the aid of a microscope for the X-ray diffraction investigations. For single crystal investigations they were mounted on the tips of thin glass fibers. Data were collected on a Bruker–Nonius Apex X8 diffractometer, equipped with a CCD detector. Measurements were carried out using monochromatic Mo Kα radiation with $\lambda = 0.71073$ Å. Preliminary data of the unit cell were obtained from the reflex positions of 12 frames, each measured in three different directions of the reciprocal space. After completion of the data measurements the intensities were corrected for Lorentz, polarization, and absorption effects using

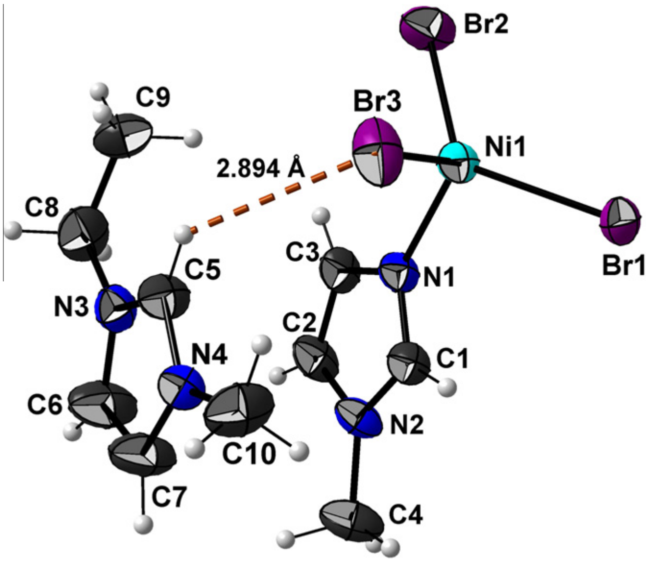

Fig. 3. Structure of one ion pair of (EMIm)[NiBr$_3$(NMIm)] in the crystal (thermal ellipsoids at 50% probability level). The dashed line shows the shortest anion–cation contact.

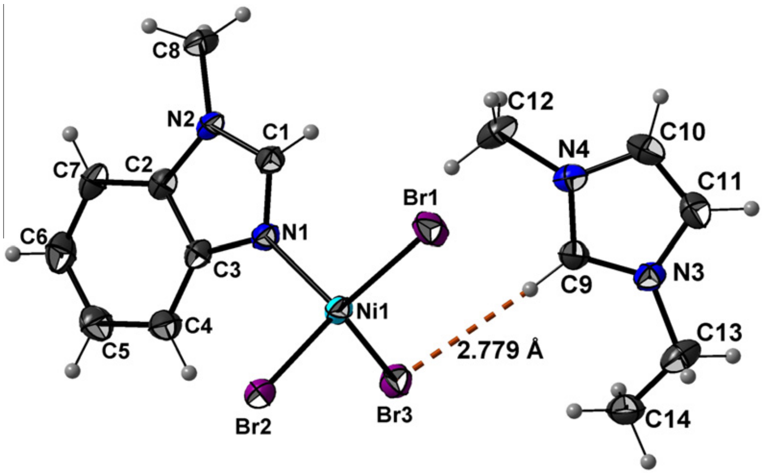

Fig. 4. Structure of one ion pair of (EMIm)[$NiBr_3$(NMBIm)] in the crystal (thermal ellipsoids at 50% probability level). The dashed line shows the shortest anion–cation contact.

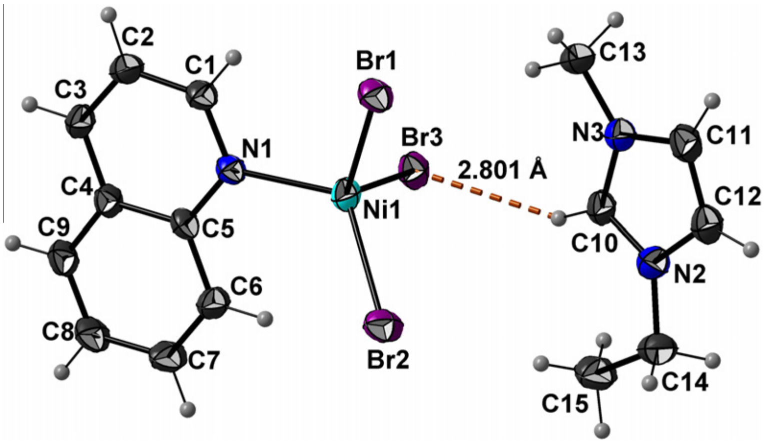

Fig. 5. Structure of one ion pair of (EMIm)[$NiBr_3$(quin)] in the crystal (thermal ellipsoids at 50% probability level). The dashed line shows the shortest anion–cation contact.

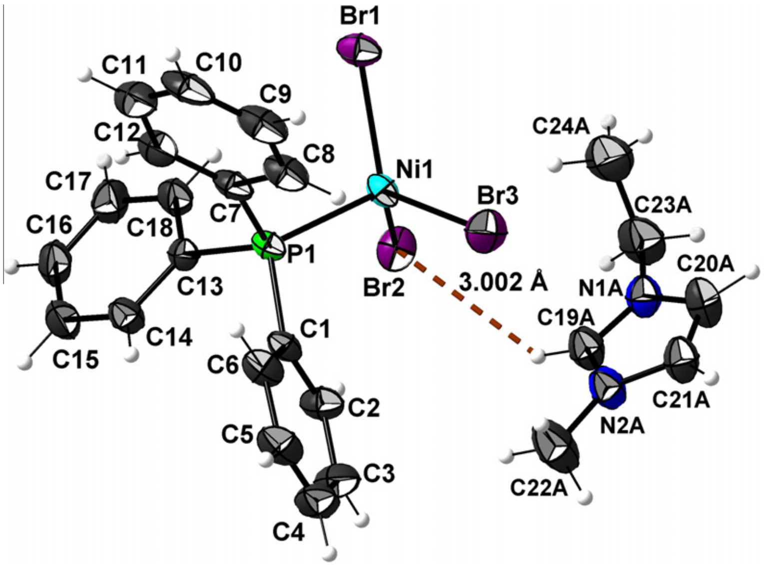

Fig. 6. Structure of one ion pair of (EMIm)[$NiBr_3(PPh_3)$] in the crystal (thermal ellipsoids at 50% probability level). The dashed line shows the shortest anion–cation contact.

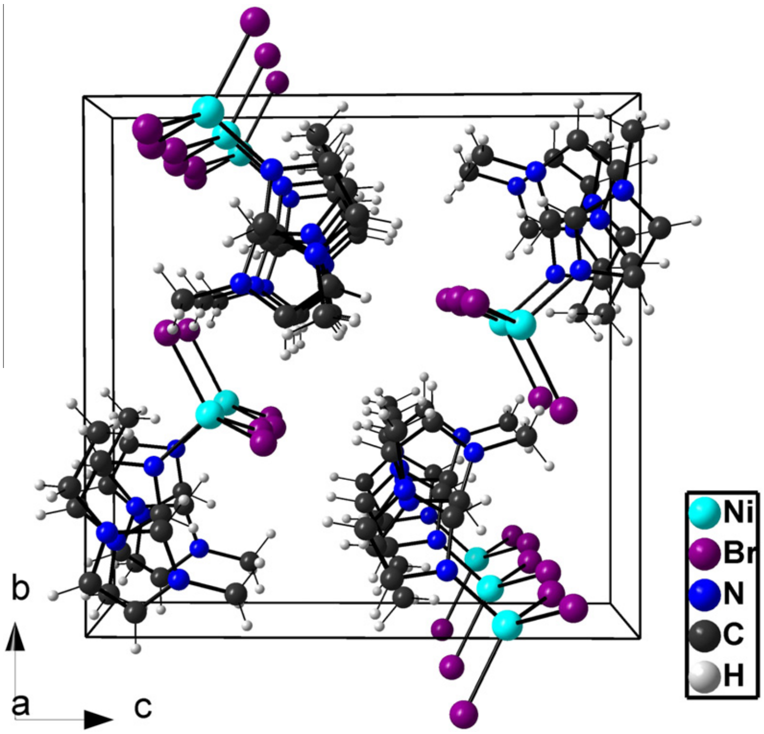

Fig. 7. Packing of the cations and complex anions in crystals of (EMIm)[$NiBr_3$(NMIm)] in a view along the *a* axis.

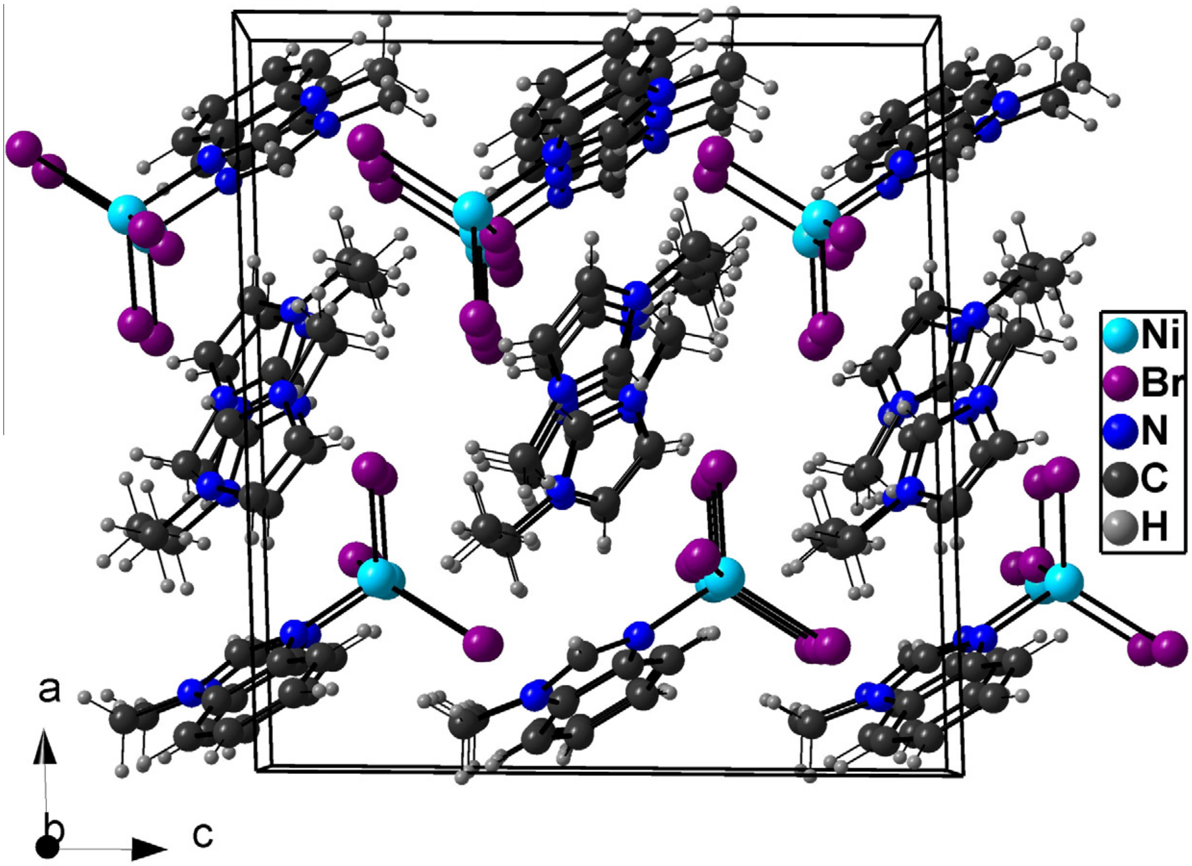

Fig. 8. Packing of the cations and complex anions in crystals of (EMIm)[$NiBr_3$(NMBIm)] in a view along the *b* axis.

the Bruker-Nonius software [11]. The structures were solved by Direct Methods using the SHELXS-97 program and refined by least-squares procedures on F^2 with the aid of the SHELXS-97 program [12].

All non-hydrogen atoms were refined anisotropically. H-atoms of all the four compounds were added on idealized positions and refined using riding models. Crystal data, data collection, and refinement parameters are compiled in Table 1.

In the structure of **3** the EMIm cation is disordered on two positions, such that the atoms of 5-membered rings are exactly on the same positions, but the methyl and the ethyl group are exchanged. This situation has been treated by a split model. The two orientations are not equally occupied; one has an occupation of 39.5(7)%, and the other one of 60.5(7)%, respectively.

2.4. Analyses and spectroscopic measurements

MIR spectra (500–4000 cm^{-1}) were recorded by using the ATR technique on a Thermo Nicolet 380 FT-IR spectrometer. Elemental analyses for C, H, and N were obtained with a Flash EA 1112 NC Analyzer from CE Instruments. UV–vis spectra were recorded using a Perkin Elmer Lambda 2 spectrometer with quartz cuvettes (Suprasil®, d = 10 mm). Melting points were determined by DSC measurements using a Mettler Toledo DSC823^e in the range of 20–200 °C with a heating rate of 10 °C/min (N_2 atmosphere, Al crucible). All melting points are peak temperatures. TG measurements were performed on a Netzsch STA 449 *F3 Jupiter*® device in the temperature range of 30–1000 °C with a heating rate of 20 °C/min in synthetic air atmosphere. Magnetic data were determined by means of ^1H NMR techniques (Evans method) [13]. Molar susceptibilities were corrected by applying Pascal constants [14]. Effective magnetic moments μ_{eff}/μ_B are given by applying the Langevin equation [15].

3. Results and discussion

3.1. Synthesis

The synthesis of complexes containing the 1-ethyl-3-methylimidazolium cation (EMIm) and the Ni^{II}-based anion $[NiBr_3(L)]^-$ (L = NMIm, NMBIm, quin, PPh_3) can be achieved in moderate to high yield by reacting (EMIm)Br, anhydrous $NiBr_2$, and L in a molar ratio of 1:1:1 in 1-butanol according to Scheme 1. All compounds of the composition (EMIm)[$NiBr_3(L)$] are distinguished by intensive violet-blue to blue-green colors in crystalline form. They are non-hygroscopic solids, which are soluble in organic solvents, especially in acetone, acetonitrile and alcohols. Suitable single crystals of the compounds (EMIm)[$NiBr_3(L)$] were obtained directly from the reaction vessels by slowly cooling to ambient temperature of saturated boiling 1-butanol solutions of the salts.

3.2. Magnetic properties

The magnetic properties at room temperature of all complex salts were determined in solution using NMR techniques by applying the Evans method [13]. The resulting data are listed in the Experimental Section. All complexes show similar magnetic properties: They are paramagnetic substances with effective magnetic moments in the range of μ_{eff} = 3.72–3.76 μ_B at 25 °C (spin only, high-spin Ni^{II}: μ_{eff} = 2.83 μ_B). These values resemble closely those of related compounds with tetrahedral $[NiX_4]^{2-}$ (X = Cl, Br) complex anions, for example, $(Et_4N)_2[NiCl_4]$: μ_{eff} = 3.87 μ_B (20 °C, [16]), $(Ph_3MeAs)_2[NiCl_4]$: μ_{eff} = 3.89 μ_B (20 °C, [16]), $(Et_4N)_2[NiBr_4]$: μ_{eff} = 3.79 μ_B (20 °C, [16]), $(DBTMIm)_2[NiBr_4]$: μ_{eff} = 3.80 μ_B (25 °C, [7c]), or pseudo-tetrahedral $[NiBr_3L]^-$ complex anions, for example, $(Et_4N)[NiBr_3(PPh_3)]$: μ_{eff} = 3.66 μ_B (27 °C, [17]), or $(^nBu_4N)[NiBr_3(quin)]$: μ_{eff} = 3.15–3.84 μ_B (22 °C, [18]). These literature values show that slight deviations of μ_{eff} from the spin-only values as found also for the title compounds are found quite often for tetrahedral complexes, as discussed for example in Ref. [25]. Because large cations separate the paramagnetic Ni(II) centers (see below) cooperative effects are expected to be non-existent. Therefore, we expect similar magnetic behavior in the solid state as in solution.

3.3. Electronic spectra

UV–vis spectra of **1**–**4** in acetonitrile show two bands in the visible wavelength regions (Table 3). These bands are characteristic for Ni(II) in tetrahedral coordination modes.

The first band at 350 (355, 372, 378) nm can be assigned to a charge-transfer-transition while the latter is at 621 (602, 649,

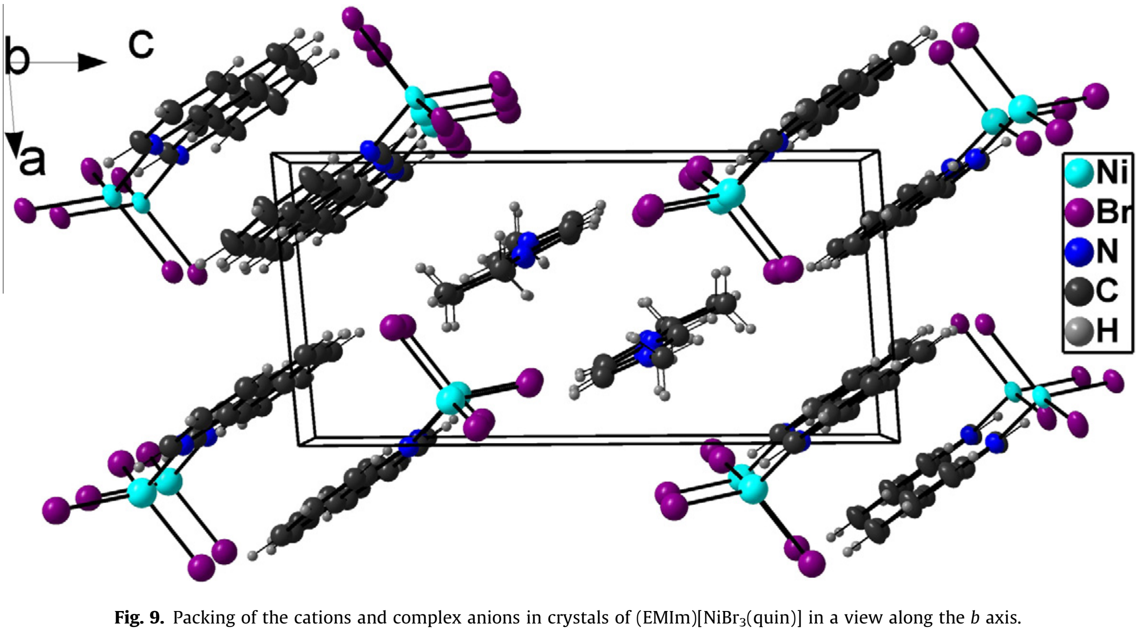

Fig. 9. Packing of the cations and complex anions in crystals of (EMIm)[$NiBr_3$(quin)] in a view along the *b* axis.

640) nm caused by d-d-transitions. These values compare well to literature known ones for known $[NiBr_3(L)]$-type complex anions as $(NEt_4)[NiBr_3(CH_3CN)]$ with absorption maxima at 372.5 and 635 nm [19] and 386 and 635 nm for $(NEt)_4[NiBr_3(PPh_3)]$ in nitromethane [4].

This d-d-transition allows the integration of the used ligands into the spectrochemical series. Thus, sorted by the extent of ligand field splitting the order is NMBIm > NMIm > PPh_3~quin.

3.4. Thermal properties

Thermal data of the four title substances have been measured using DSC and TGA techniques. Melting points were detected by applying DSC measurements (20–200 °C) as endothermic peaks between 100 and 170 °C. All melting points are listed in the Experimental Section and the melting point is increasing with increasing molar mass of the ligand from 110 °C in $(EMIm)[NiBr_3(NMIm)]$ (NMIm: $M = 82.10$ g/mol) to 168 °C in $(EMIm)[NiBr_3(PPh_3)]$ (PPh_3: $M = 262.29$ g/mol). All compounds are stable in the liquid state below 200 °C even under air before thermal degradation occurs. The decomposition curves of $(EMIm)[NiBr_3(L)]$ in air in the temperature range of 30–1000 °C are depicted in Fig. 1. From Fig. 1 it can be seen, that the decomposition of $(EMIm)[NiBr_3(L)]$ follows complex pathways, while decomposition in air starts at 250–300 °C, followed by a short horizontal in the temperature range of 450–550 °C, and further decomposition until 1000 °C leaving a complex mixture of Ni and NiO. Interestingly, the lowest melting complexes $(EMIm)[NiBr_3(NMIm)]$ and $(EMIm)[NiBr_3(NMBIm)]$ show the highest degradation temperatures (~300 °C) suggesting liquid ranges for these two compounds of almost 200 °C. This behavior is also observable by isothermal TGA measurements at 200 °C. Fig. 2 shows additional TGA curves for $(EMIm)[NiBr_3(L)]$ for isothermal measurements in air over a longer period of time at 200 °C (7 h). Even after 7 h at 200 °C only a mass loss of approximately 6 % can be detected for the lowest melting substance $(EMIm)[NiBr_3(NMIm)]$, while the highest melting salt $(EMIm)[NiBr_3(PPh_3)]$ loses more than 15% of its mass. From Figs. 1 and 2 it can be concluded, that the rate of decomposition of $(EMIm)[NiBr_3(L)]$ is highly dependent on the chosen ligand *L*. This behavior is qualitatively explained on the basis of the extended hydrogen bonding networks and further discussed in the Crystal Structures Section.

3.5. Crystal and molecular structures

In the course of our investigations of mono-anionic transition metal complex ions as candidates for new Ionic Liquids, we determined the single crystal X-ray structures of the four new title compounds. Crystal data and parameters of the structure determinations and refinements are listed in Table 1, and selected bond lengths and angles in Table 2. All four compounds consist of isolated 1-ethyl-3-methylimidazolium cations and $[NiBr_3(L)]^-$ anions, i.e. the compounds are to be described as salts.

The coordination geometry around the Ni atoms in **1**–**3** is pseudo-tetrahedral $NiBr_3N$ with 3 bromido ligands and 1 N ligand atom from the corresponding aromatic organic N ligand (NMIm, NMBIm,

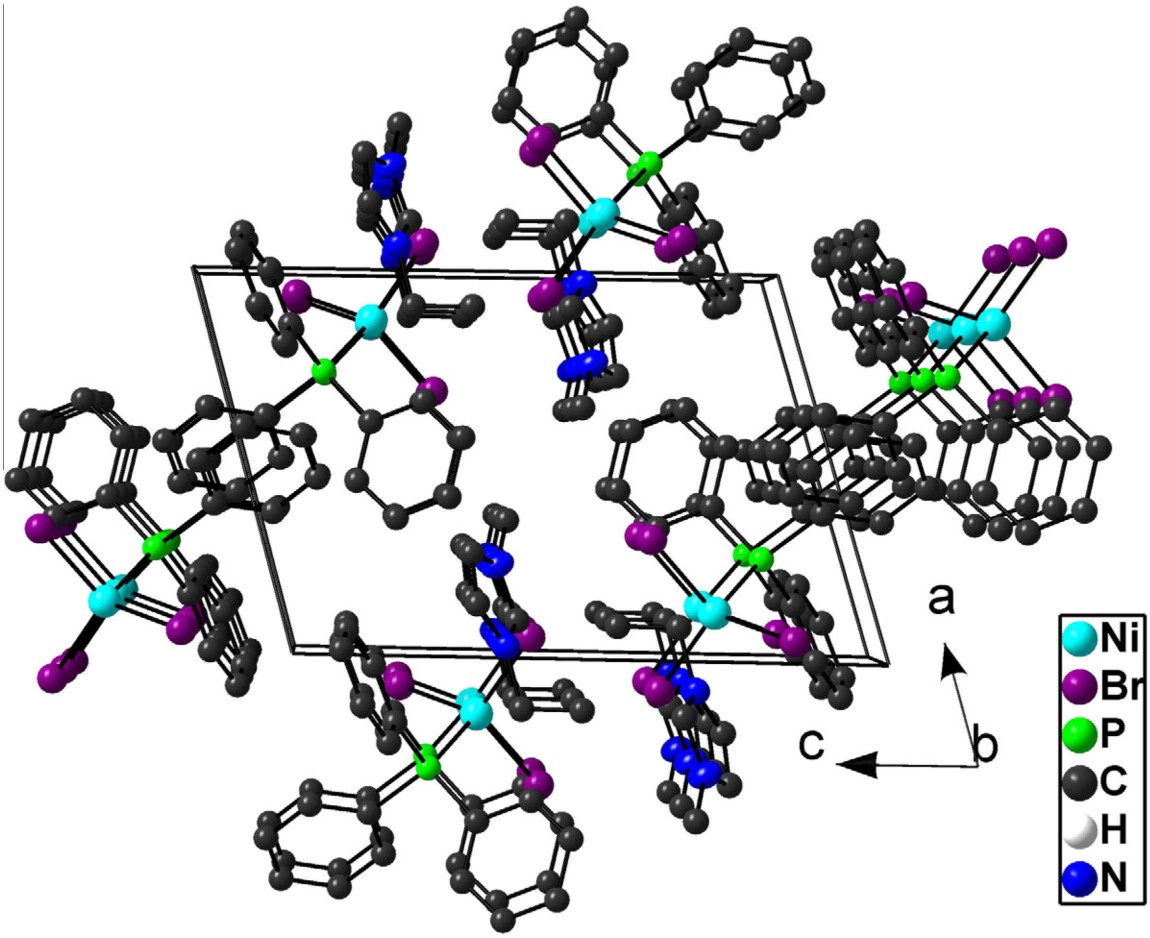

Fig. 10. Packing of the cations and complex anions in crystals of $(EMIm)[NiBr_3(PPh_3)]$ in a view along the *b* axis. H atoms are omitted for clarity. Only one orientation of the disordered EMIm cation is shown.

and quin). In **4**, with $L = PPh_3$ the Ni coordination is $NiBr_3P$, respectively. The average Ni–Br and the Ni–N/Ni–P bond distances fall in their expected regions (see Table 2). In **1** and **2** with the principally similar ligands NMIm and NMBIm the values are almost identical. The Ni–Br distance in **3** (quin ligand) compares also well with the ones of the former two compounds, but the Ni–N distance is slightly longer. To the best of our knowledge crystal structure data of nickel complex salts with ligands comparable to those of 1,2, or 3 exist in the literature so far only for $(^nBu_4N)[NiBr_3(quin)]$ [20]. The structural parameters of this compound compare well with those of **3**. Also, the bond lengths of the anion of **4** are in the same range as those of $(Ph_4As)[NiBr_3(PPh_3)]$ [21].

In all four title compounds the average Br–Ni–Br angles are larger than the ideal tetrahedral value, whereas the average Br–Ni–N/P angles are smaller than 109.47°, as expected from the different atom radii (see Table 2).

The salts **1** and **2** crystallize in the monoclinic crystal system, **1** with space group $P2_1/n$ and **2** with $P2_1/c$, both with four ion pairs in the unit cell. **3** and **4** crystallize triclinic ($P\bar{1}$) with two formula units in the unit cell. In all four structures the atoms of the ion pairs of the asymmetric unit are located on general positions. Therefore, none has higher point symmetry than identity. Figs. 3–6 show ORTEP plots of one ion pair of the four title compounds.

The arrangement of ions in the unit cells of **1**–**4** is shown in Figs. 7–10.

In crystals of **1** the cations and anions are alternatively stacked along the crystallographic *a* direction in such a way that the planar imidazolium rings, which are present in both the cation and the anion are arranged almost parallel. Even though, the distance of this planar units is short at 3.87 Å, π-stacking interactions are not expected to be present to a larger extend, because the five-membered ring of the cation is shifted away from that of the anion in a direction parallel to the ring plane, see Fig. 7. Also, the ring plane of the cation is tilted by 4° relative to that of the anion.

In the salt with the *N*-methylbenzimidazole ligand the arrangement of ions can also be described in such a way that rows of ions exist. But different to the arrangement in **1**, where rows of alternating cations and anions exist, here rows of only cations neighboring those of anions run along *b*. As for **1**, π-stacking interactions do not seem to play a larger role for the interaction of the ionic entities. Within *b*-*c* layers either only cations or only anions exist, i.e. layers of the EMIm cation alternate along *a* with layers of the complex anion, see Fig. 8.

The packing of ions in crystals of **3** differs significantly from that of **1** or **2**. Again, rows of cations and anions penetrate the crystal in the *b* direction, but for **3** these are double rows, with each cation and anion strand runs in a zigzag fashion along *b*, see Fig. 9.

This structural feature of rows of the same ion type is also present in **4**, where the complex anions, which is relatively large in size, compared to the ones of **1**–**3**, are arranged along the *b* direction, as are the cations, see Fig. 10. In crystals of **4** the EMIm cation is disordered with two different orientations. The positions of the imidazolium ring atoms are the same for both orientations, but the methyl group is exchanged by the ethyl group in the other orientation. The relative occupancy is 0.395/0.605.

In this type of compounds the understanding of the relation of structure/ionic arrangement with respect to the macroscopic properties like melting point, viscosity and others, is an ongoing challenge. With this respect hydrogen bonding is discussed quite often. Even though hydrogen bonding is (usually) an attractive force, increasing melting points and viscosities, in some classes of especially ionic liquids hydrogen bonding is discussed not to be responsible for higher, but for lower melting points through disturbance of the otherwise regular Coulomb system [22–24]. In the four salts of this investigation one especially acidic proton is present in the EMIm cation, attached to the C atom bonded to the two N atoms (H at C5 (**1**), C9 (**2**), C10 (**3**), and C19 (**4**)). All these H atoms have rather short distances to Br atoms of neighboring complex anions. They range from 2.779 Å in **2** to 3.002 Å in **4**. Unfortunately, the trend of these increasing hydrogen bond lengths does not reflect any reasonable trend of melting points of these compounds.

4. Conclusion

Results of detailed investigations about new compounds with pseudo-tetrahedral Nickel(II) complex anions of the type $[NiBr_3(L)]^-$ with *L* = organic ligand N ligands (three examples) and one example with a P ligand is presented. Information about the synthesis, single-crystal X-ray structures, spectroscopy, thermal behavior and magnetic properties of $(EMIm)[NiBr_3(L)]$ with *L* = *N*-methylimidazole, *N*-methylbenzimidazole, quinoline, and triphenylphosphane; EMIm = 1-ethyl-3-methylimidazolim is given. They all contain pseudo-tetrahedrally coordinated Nickel ions. The materials are paramagnetic and thermally stable up to 200 °C. They have relatively low melting points, and might be useful as molten salts.

Acknowledgment

Support from the Deutsche Forschungsgemeinschaft (SPP 1191) is gratefully acknowledged.

Appendix A. Supplementary data

CCDC 878295, 878294, 878293 and 878296 contains the supplementary crystallographic data for compounds **1**–**4**. These data can be obtained free of charge via http://www.ccdc.cam.ac.uk/conts/retrieving.html, or from the Cambridge Crystallographic Data Centre, 12 Union Road, Cambridge CB2 1EZ, UK; fax: (+44) 1223-336-033; or e-mail: deposit@ccdc.cam.ac.uk.

References

[1] a) S.A. Kozlova, S.P. Verevkin, A. Heintz, T. Peppel, M. Köckerling, J. Chem. Eng. Data 54 (2009) 1524;
b) T. Peppel, M. Köckerling, Z. Anorg. Allg. Chem. 636 (2010) 2439;
c) T. Peppel, M. Köckerling, M. Geppert-Rybczyńska, R.V. Ralys, J.K. Lehmann, S.P. Verevkin, A. Heintz, Angew. Chem. 122 (2010) 7270–7274. Angew. Chem. Int. Ed. 49 (2010), 7116;
d) T. Peppel, C. Schmidt, M. Köckerling, Z. Anorg. Allg. Chem. 637 (2011) 1314.
[2] a) S. Hayashi, H. Hamaguchi, Chem. Lett. 33 (2004) 1590;
b) Q.-G. Zhang, J.-Z. Yang, X.-M. Lu, J.-S. Gui, M. Huang, Fluid Phase Equilib. 226 (2004) 207;
c) S. Hayashi, S. Saha, H. Hamaguchi, IEEE Trans. Magn. 42 (2006) 12;
d) C. Zhong, T. Sasaki, A. Jimbo-Kobayashi, E. Fujiwara, A. Kobayashi, M. Tada, Y. Iwasawa, Bull. Chem. Soc. Jpn. 80 (2007) 2365;
e) M. Okuno, H. Hamaguchi, S. Hayashi, Appl. Phys. Lett. 89 (2006) 132506;
f) M.H. Valkenberg, C. De Castro, W.F. Holderich, Appl. Catal. A215 (2001) 185;
g) Y. Jiang, C. Guo, H. Liu, China Particuol. 5 (2007) 130.
[3] B.N. Thakura, R.S. Prasadab, N.K. Jhaa, E.E. Alic, Synth. React. Inorg. Met.-Org. Chem. 18 (1988) 197.
[4] C.D. Burbridge, D.M.L. Goodgame, J. Chem. Soc. A 5 (1968) 1074.
[5] a) I. Bertini, D. Gatteschi, F. Mani, Inorg. Chim. Acta 7 (1973) 717;
b) A. Bencini, D. Gatteschi, Inorg. Chem. 16 (1977) 2141;
c) M. Gerloch, L.R. Hanton, Inorg. Chem. 19 (1980) 1692;
d) A. Bencini, C. Benelli, D. Gatteschi, C. Zanchini, J. Mol. Struct. 60 (1980) 401;
e) T.-T. Pan, D.-J. Xu, Acta Cryst. E60 (2004) m56.
[6] a) W. De, W. Horrocks Jr., D.H. Templeton, A. Zalkin, Inorg. Chem. 7 (1968) 2303;
b) M.K. Misra, D.V. Ramana, J. Organomet. Chem. 22 (1970) 227;
c) M. Gerloch, L.R. Hanton, M.R. Manning, Inorg. Chim. Acta 48 (1981) 205;
d) J. Yang, I. Del Rosal, M. Fasulo, P. Sangtrirutnugul, L. Maron, T.D. Tilley, Organometallics 29 (2010) 5544.
[7] J.M. Savariault, J. Galy, J. Mol. Struct. 176 (1988) 313.
[8] W. Wang, X. Zhang, D. Huang, H. Zhu, C. Chen, Q. Liu, Acta Cryst. E57 (2001) m561.
[9] T. Peppel, M. Köckerling, Cryst. Growth Des. 11 (2011) 5461.
[10] B. Pilarski, Liebigs Ann. Chem. 6 (1983) 1078.

[11] Bruker-Nonius Inc., Apex-2, v. 1.6-8, Saint, v. 6.25a, SADABS – Software for the CCD detector System, Madison, WI, USA, 2003.
[12] G.M. Sheldrick, Acta. Cryst. A64 (2008) 112.
[13] a) D.F. Evans, J. Chem. Soc. (1959) 2003;
b) S.K. Sur, J. Magn. Reson. 82 (1989) 169.
[14] a) A. Pacault, J. Hoarau, A. Marchand, Adv. Chem. Phys. 3 (1960) 171;
b) W. Haberditzl, Angew. Chem. 78 (1966) 277.
[15] a) P. Langevin, J. Phys. 4 (1905) 678;
b) P. Langevin, Ann. Chim. Phys. 5 (1905) 70.
[16] N.S. Gill, R.S. Nyholm, J. Chem. Soc. (1959) 3997.
[17] F.A. Cotton, D.M.L. Goodgame, J. Am. Chem. Soc. 82 (1960) 2967.
[18] M. Gerloch, L.R. Hanton, Inorg. Chem. 19 (1980) 1692.
[19] W. Libus, W. Grzybkowski, Electrochim. Acta 23 (1977) 791.
[20] W. De, W. Horrocks Jr., D.H. Templeton, A. Zalkin, Inorg. Chem. 7 (1968) 2303.
[21] L.R. Hanton, P.R. Raithby, Acta Crystallogr., Sect. B 36 (1980) 2417.
[22] T. Peppel, C. Roth, K. Fumino, D. Paschek, M. Köckerling, R. Ludwig, Angew. Chem. 123 (2011) 6791. Angew. Chem., Int. Ed. 50 (2011), 6661.
[23] C. Roth, T. Peppel, K. Fumino, M. Köckerling, R. Ludwig, Angew. Chem. 122 (2010) 10419. Angew. Chem., Int. Ed. 49 (2010), 10221..
[24] K. Fumino, T. Peppel, M. Geppert-Rybczyńska, D.H. Zaitsau, J.K. Lehmann, S.P. Verevkin, M. Köckerling, R. Ludwig, Phys. Chem. Chem. Phys. 13 (2011) 14064.
[25] B.N. Figgis, J. Lewis, The Magnetochemistry of Complex Compounds, in: J. Lewis, R.G. Wilkins (Eds.), Modern Coordination Chemistry, Wiley, New York, 1960.